PHYSICAL REVIEW C VOLUME 50, NUMBER 2 AUGUST 1994

Multiple band structures at high angular momentum in ^{115}I: Towards unfavored band termination

E. S. Paul
Oliver Lodge Laboratory, University of Liverpool, PO Box 147, Liverpool L69 3BX, United Kingdom

H. R. Andrews, V. P. Janzen, D. C. Radford, and D. Ward
Chalk River Laboratories, AECL Research, Chalk River, Ontario, K0J 1J0, Canada

T. E. Drake and J. DeGraaf
Department of Physics, University of Toronto, Toronto, Ontario M5S 1A7, Canada

S. Pilotte
Department of Physics, University of Ottawa, Ottawa K1N 6N5, Canada

I. Ragnarsson
Department of Mathematical Physics, Lund Institute of Technology, PO Box 118, S-22100, Lund, Sweden
(Received 24 March 1994)

Six new rotational bands have been established in ^{115}I at high spin using the near symmetric ^{60}Ni(^{58}Ni,$3p\gamma$) reaction at 250 MeV. Several of the bands are observed to frequencies beyond $\hbar\omega$=1.0 MeV (spin approaching 50$\hbar$). All the bands show a characteristic drop off in their dynamic moments of inertia with increasing spin. The low values at the highest spins are consistent with predictions for a band termination in which a gradual shape change from collective prolate to noncollective oblate occurs over many transitions. These smoothly occurring terminations contrast with the abrupt "favored" terminations previously observed in this and other odd-A iodine nuclei.

PACS number(s): 21.10.Re, 27.60.+j, 23.20.Lv, 25.70.Hi

I. INTRODUCTION

Nuclei near the $Z = 50$ closed proton shell have revealed exotic collective structures, which coexist with the expected single-particle properties. Recently, rotational "intruder bands," extending to both high spin and excitation energy, have been observed. These bands have been found in several odd-A antimony ($Z = 51$) isotopes ranging from ^{109}Sb to ^{117}Sb [1–5], in addition to several even tin nuclei, e.g., ^{108}Sn [6]. The systematics have been extended to $Z = 52, 53$ nuclei with data from the Eurogam array [7].

The present investigation populated states in ^{115}I ($Z = 53$) at high angular momentum and led to the observation of several similar rotational band structures extending to extremely high frequencies beyond $\hbar\omega$=1.0 MeV (spin approaching 50$\hbar$). A unique feature of these bands, also evident in some of the neighboring nuclei [2,6,7], is a stretching out of the γ-ray energy spacings with increasing spin. This effect leads to a fall off in their dynamic moments of inertia with increasing rotational frequency such that unusually low values of the moment of inertia are observed at high spin, much lower than the rigid-body estimate. These novel features are suggested to arise from a band termination in which the nucleus traces a gradual path through the γ plane from a collective prolate shape ($\gamma = 0°$) to the noncollective oblate shape ($\gamma = +60°$) over many transitions. During this slow shape transition, the single-particle angular momenta of the valence particles (outside the $N = Z = 50$ core) are gradually aligned with the "rotation" axis. The final energetically unfavored terminating states reside well above yrast. This behavior is to be contrasted with the abrupt favored termination seen in several neighboring nuclei in this mass region, e.g., the $43/2^-$ and $51/2^-$ yrast states in this nucleus [8] and similar states in odd-A $^{117-121}$I [9–13]. Theoretical results are presented in order to assign specific configurations to the new bands in ^{115}I.

II. EXPERIMENTAL DETAILS AND RESULTS

High-spin states in ^{115}I were populated with the ^{60}Ni(^{58}Ni,$3p$)^{115}I reaction at a bombarding energy of 250 MeV. The target consisted of two self-supporting foils of ^{60}Ni, each of nominal thickness 480 μg/cm^2. The ^{58}Ni heavy-ion beam was provided by the Tandem Accelerator Superconducting Cyclotron (TASCC) facility at the Chalk River Laboratories. Coincident γ-γ data were acquired with the 8π spectrometer, which consists of 20 Compton-suppressed HPGe detectors plus a 71-element BGO inner-ball calorimeter which provides γ-ray sum-energy H and fold, K, information. The gains of the HPGe detectors were matched off-line with an ^{88}Y radioactive source, and were adjusted on-line for a recoil velocity $v/c = 4.45\%$. Data were written onto magnetic tape for events in which two or more suppressed HPGe detectors registered in prompt time coincidence with 10 or more elements of the inner ball (fold $K \geq 10$). Under this condition, approximately 3.3×10^8 events were recorded to tape.

In the off-line analysis for ^{115}I ($3p$ channel), only events with a total sum-energy $H \geq 13.4$ MeV were incremented into a symmetrized $E_\gamma - E_\gamma$ matrix. Under this condition approximately 50% of the recorded data were replayed into this high-H matrix. The high sum-energy condition greatly suppressed events from the competing 4- and 5-particle evaporation channels which have lower average H and K distributions relative to the 3-particle channels. A second, low-H, matrix was constructed for events with a total sum-energy in the range $7.0\leq H \leq 12.2$ MeV in order to enhance the relative yields of, and allow the study of, other residual nuclei produced in the ^{58}Ni + ^{60}Ni reaction.

The matrices were analyzed with the ESCL8R program [14], with the important results being the observation of 10 cascades of transitions extending to high γ-ray energy, and hence rotational frequency. Eight of the bands have been observed for the first time. Six were found in the high-H matrix and are assigned to ^{115}I through coincidences with the known transitions [8]. One of the shorter bands has been connected to the top of the yrast states in ^{115}I. Four further bands were observed in the low-H matrix: one band had already been established in ^{112}Te (α2p channel) from recent Eurogam data [7], a second had previously been established in ^{111}Sb (α3p) [3], while the third and fourth have very recently been assigned to ^{111}Sb from data obtained with the gammasphere spectrometer [15]. This paper will concentrate on the six bands assigned to ^{115}I. Gated coincidence spectra of five of the bands are shown in Fig. 1, while the sixth band is presented in Fig. 2 which shows the top of the level scheme of ^{115}I. The transition energies are listed in Table I. The maximum intensities of bands 1–5 are estimated to be ~ 1% of the channel strength; this weakness precludes the firm establishment of linking transitions into the known ^{115}I levels. However, the observation of weak coincidences with the known levels yields a lower limit of I ~ 35/2 for the lowest level of each band. Band 6 is much stronger with a maximum intensity of ~ 10%.

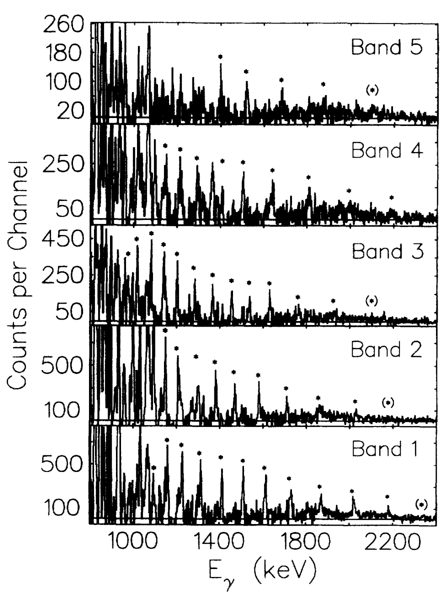

FIG. 1. Coincidence spectra showing five bands assigned to ^{115}I. These spectra were obtained by summing several of the individual gates for each band. The positions of the band members are indicated by the stars, while their energies are listed in Table I.

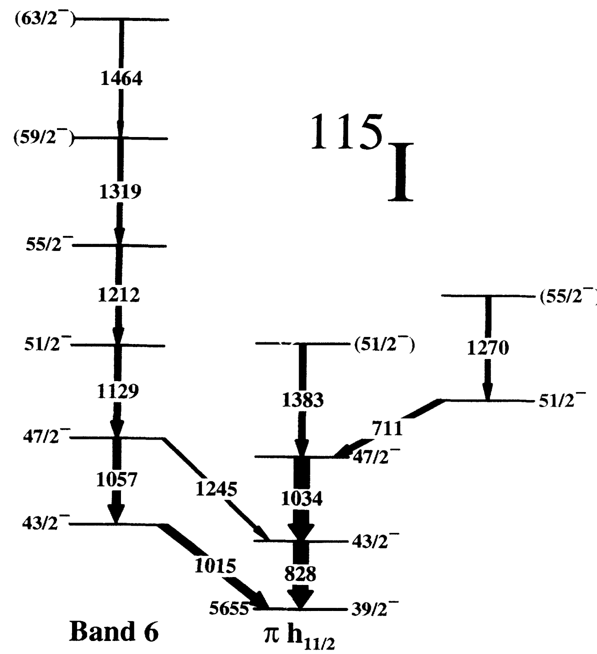

FIG. 2. Decay scheme for ^{115}I above the $39/2^-$ member (excitation energy of 5655 keV) of the $\pi h_{11/2}$ band [8]. Band 6 is shown to the left. Some transition multipolarities have been deduced from an angular correlation analysis of the γ-γ coincidence data.

TABLE I. Gamma-ray transition energies (keV) for the six new bands in ^{115}I. The energies are estimated to be accurate to ±1 keV.

Band 1	Band 2	Band 3	Band 4	Band 5	Band 6
1093	981	923	(1146)	1395	1057
1157	1030	969	1204	1517	1129
1226	1090	1017	1292	1680	1212
1311	1146	1081	1402	1879	1319
1410	1209	1136	1500	(2099)	1464
1507	1300	1201	1639		
1611	1383	1283	1810		
1728	1465	1365	1997		
1870	1579	1451	(2188)		
2019	1705	1533			
2178	1859	1631			
(2339)	2025	1760			
	(2190)	1925			
		(2116)			

III. DISCUSSION

Since the spins of the bands are unknown (except for the strong band 6), it is appropriate to discuss dynamic moments of inertia, $\mathcal{J}^{(2)} = dI/d\omega \approx 4/\Delta E_\gamma$, which can be derived without a knowledge of level spins. The experimental dynamic moments of inertia, extracted for the six new bands in ^{115}I are shown in Fig. 3(a), while theoretical moments of inertia are shown in Fig. 3(b) for various single-particle configurations (see below). The experimental values all show a rapid decrease in moment of inertia with increasing frequency; above a rotational frequency $\omega \sim 0.8$ MeV/$\hbar$, the values fall below the rigid-body estimate for a prolate nucleus with quadrupole deformation $\varepsilon_2 = 0.25$.

A. Theoretical calculations

In order to interpret the structure of the new bands, calculations based on a modified oscillator potential with no pairing have been performed according to the formalism described in Ref. [16]. These calculations predict states at a given spin with minimized shape parameters (ε_2, ε_4, γ) for various single-particle configurations described by the number of particles with signature $\alpha = +1/2$ and $\alpha = -1/2$, respectively, in the different N shells. Furthermore, for ^{115}I we have succeeded in putting labels on the high-j orbitals so that the numbers

TABLE II. Calculated terminating spins for some configurations. The dominant high-j components are shown. The remaining valence particles reside in N=4 orbitals.

(Parity, Signature)	Dominant structure			Terminating spin
$(+,+1/2)_1$	$\pi h_{11/2}$	$\otimes$	$\nu h^3_{11/2}$	$73/2^+$
$(+,+1/2)_2$	$\pi g^{-2}_{9/2} h^2_{11/2}$	$\otimes$	$\nu h^4_{11/2}$	$109/2^+$
$(+,+1/2)_3$	$\pi g^{-1}_{9/2} h^2_{11/2}$	$\otimes$	$\nu h^4_{11/2}$	$97/2^+$
$(+,-1/2)_1$	$\pi h_{11/2}$	$\otimes$	$\nu h^3_{11/2}$	$71/2^+$
$(+,-1/2)_2$	$\pi g^{-1}_{9/2} h^2_{11/2}$	$\otimes$	$\nu h^4_{11/2}$	$95/2^+$
$(-,+1/2)_1$	$\pi g^{-1}_{9/2} h^2_{11/2}$	$\otimes$	$\nu h^3_{11/2}$	$89/2^-$
$(-,-1/2)_1$	$\pi h_{11/2}$	$\otimes$	$\nu h^2_{11/2}$	$63/2^-$
$(-,-1/2)_2$	$\pi h_{11/2}$	$\otimes$	$\nu h^4_{11/2}$	$79/2^-$
$(-,-1/2)_3$	$\pi g^{-2}_{9/2} h^2_{11/2}$	$\otimes$	$\nu h^3_{11/2}$	$103/2^-$

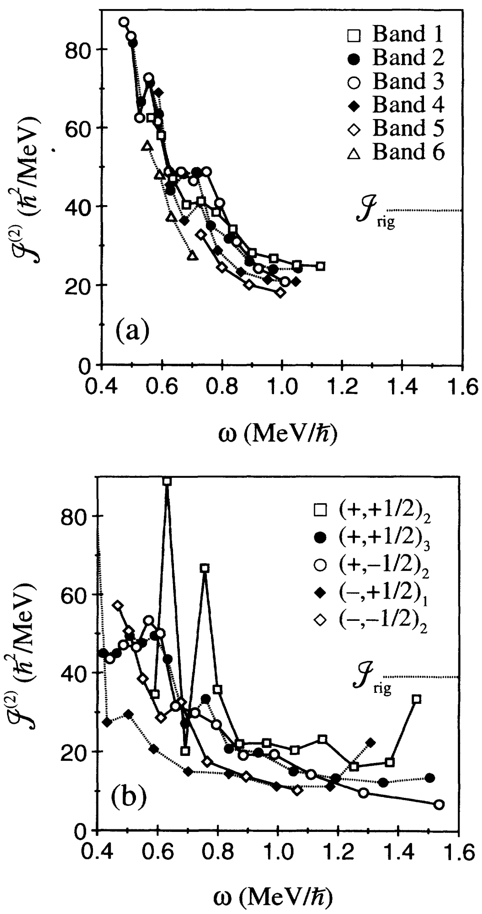

FIG. 3. Experimental dynamic moments of inertia (a) for the six bands in ^{115}I. The rigid body estimate is also shown for a prolate nucleus with quadrupole deformation $\varepsilon_2 = 0.25$. Theoretical dynamic moments of inertia (b) for five of the configurations of Table II. The configurations are classified by parity and signature quantum numbers.

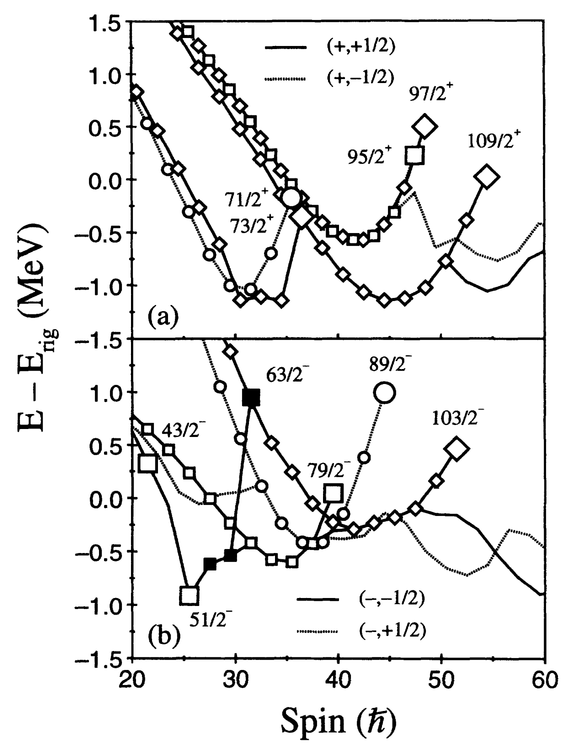

FIG. 4. Calculated energies of states in ^{115}I, minus a rigid-rotor reference, plotted as a function of spin. Positive-parity configurations are shown in (a) and negative parity configurations in (b). The points represent specific configurations as given in Table II. The lines connect states of the same signature and parity and do not necessarily follow a band sequence. Those lines without points follow the locus of yrast states, of a given signature and parity. The terminating spins (at $\gamma = +60°$) are labeled. With the exception of the $43/2^-$ and $51/2^-$ yrast states, they represent "unfavored" terminating states.

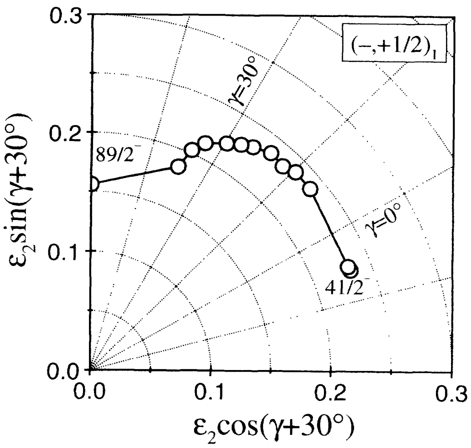

FIG. 5. Shape evolution of the $(-,+1/2)_1$ configuration (see Table II) from prolate to oblate. The points are separated by $2\hbar$. The final terminating state at $\gamma = +60°$ has $I^\pi = 89/2^-$.

of high-j particles can be specified. Thus, we can keep track of the protons in $g_{9/2}$ orbitals and in the other $N = 4$ orbitals $(g_{7/2}, d_{5/2})$ independently. Results are presented in Table II and Figs. 3(b), 4, and 5, where we use a simple classification, specifying only parity and signature quantum numbers. The calculations indicate a gradual shape change through the γ plane over many transitions until final termination is reached at the noncollective $\gamma = +60°$ shape. The high-j configurations are given in Table II; the other valence particles outside the $N = Z = 50$ shell closure reside in N=4 orbitals: namely, $\pi g_{7/2}$, $d_{5/2}$, and $\nu g_{7/2}$, $d_{5/2}$, $d_{3/2}$ orbitals. In Table II, the highest spin possible with no $d_{3/2}$ neutrons is also given. The energies of the configurations in Table II, minus a rigid-rotor reference, are plotted as a function of spin in Fig. 4. Since the states are not yrast as the terminating state is reached, and since the last spins before the termination are energetically expensive, it is appropriate to classify this form of band termination as unfavored. Figure 5 shows an example of the shape evolution from collective prolate ($\gamma = 0°$) to noncollective oblate ($\gamma = +60°$) for one of the configurations listed in Table II, namely the $(-,+1/2)_1$ configuration. It can be seen that a gradual shape change takes place over many transitions, with γ increasing and ε_2 decreasing near termination. Final termination is achieved at $I^\pi = 89/2^-$.

Theoretical dynamic moments of inertia for five of the configurations in Table II are shown in Fig. 3(b) where they can be compared to experimental values. The values are again much lower than the rigid-body estimate at high rotational frequencies and there is a qualitative agreement with experiment. These configurations will be discussed in more detail in the following sections.

B. Band 6

In order to interpret the new band structures in ^{115}I, it is easiest to start with band 6 which is connected to the known yrast levels in Fig. 2. One possibility is that band 6 represents an aligned $\pi h_{11/2} \otimes \nu h^2_{11/2}$ structure since similar structures are observed in ^{117}I [9] and ^{119}I [12] at high spin. It is interesting to note that the highest spin observed in this band is the maximum spin for the configuration (relative to the $N = Z = 50$ doubly-magic core) $\pi\left(g_{7/2}d_{5/2}\right)^2_{6^+}\left(h_{11/2}\right)^1_{11/2^-} \otimes \nu\left(g_{7/2}d_{5/2}\right)^{10}_{10^+}\left(h_{11/2}\right)^2_{10^+}$. In the calculations of Fig. 4(b) the corresponding configuration is yrast for $I^\pi = 55/2^-$ and $59/2^-$. The $63/2^-$ state of band 6 may thus represent the termination of this configuration into an unfavored, i.e. nonyrast, noncollective oblate state at $\gamma = +60°$. With regard to the states shown in the center and right of Fig. 2, the yrast $43/2^-$ and $51/2^-$ states lie unusually low and have previously been interpreted as favored yrast noncollective oblate states [8]. The $43/2^-$ state, which has been systematically observed in the light iodine isotopes, is built on the $\pi\left(g_{7/2}d_{5/2}\right)^2_{6^+}\left(h_{11/2}\right)^1_{11/2^-} \otimes \nu\left(g_{7/2}\right)^8_{0^+}\left(d_{5/2}\right)^2_{0^+}\left(h_{11/2}\right)^2_{10^+}$ configuration in ^{115}I. The $51/2^-$ state is clearly seen as yrast in the calculations of Fig. 4(b) and has the configuration $\pi(g_{7/2}d_{5/2})^2_{6^+}(h_{11/2})^1_{11/2^-} \otimes \nu(g_{7/2})^8_{0^+}(d_{5/2})^2_{4^+}(h_{11/2})^2_{10^+}$.

C. Bands 1–5

Experimentally, band 1 has the highest moment of inertia of the new bands, and is seen to the highest frequencies. This is consistent with the $(+,+1/2)_2$ configuration of Table II which is yrast for $36 \le I \le 50\hbar$ [see Fig. 4(a)]. The full microscopic structure is $\pi\left(g_{7/2}d_{5/2}\right)^3\left(g_{9/2}\right)^{-2}\left(h_{11/2}\right)^2 \otimes \nu\left(g_{7/2}d_{5/2}\right)^8\left(h_{11/2}\right)^4$; this configuration can carry a maximum spin of 109/2. An analogous structure has been proposed for a similar band in ^{113}I [7]. Experimentally, bands 2 and 3 have the next largest moments of inertia, which are similar to each other. Theoretically, these bands might be explained by the $(+,+1/2)_3$ and $(+,-1/2)_2$ configurations of Table II which are signature partners based on the $\pi\left(g_{7/2}d_{5/2}\right)^2\left(g_{9/2}\right)^{-1}\left(h_{11/2}\right)^2 \otimes \nu\left(g_{7/2}d_{5/2}\right)^8\left(h_{11/2}\right)^4$ configuration. The three positive-parity configurations, suggested for bands 1–3, all involve the promotion of one or more $g_{9/2}$ protons across the $Z = 50$ shell gap.

Bands 4 and 5 have the lowest moments of inertia and are seen at high frequencies. They might be associated with the $(-,+1/2)_1$ and $(-,-1/2)_2$ configurations of Table II. There is no experimental evidence for bands corresponding to the $(+,+1/2)_1$ and $(+,-1/2)_1$ configurations of Table II, i.e. for bands other than band 6 which are favored at low spin and terminate at moderate spins; the $(+,+1/2)_1$ and $(+,-1/2)_1$ configurations are predicted to be yrast for spins $26\hbar \le I \le 36\hbar$. It should be emphasized, however, that all assignments are highly uncertain and that besides the configurations of Table II and Fig. 4, there are more bands calculated to be close to yrast. If the spins of the bands could be determined to within $\pm 2\hbar$, the detailed assignments would be made much easier.

Unfortunately, the weak bands in ^{115}I could not be followed experimentally to full termination; comparison with theory suggests that two or three more transitions are needed to achieve full termination. Similar band structures have been observed in ^{109}Sb [2] and in this case the final terminating states may have been identified. Five similar bands have also been established in neighboring ^{113}I from Eurogam data [7]. Again low dynamic moments of inertia at extremely high rotational frequencies are consistent with the present interpretation.

IV. CONCLUSION

Six rotational bands extending to high rotational frequencies and spin have been established in ^{115}I. The bands are interpreted in terms of a band termination scenario where a gradual, smooth shape change from prolate to oblate occurs over many transitions leading to the observation of "rotational" structures. This "unfavored" form of band termination is to be contrasted with the abrupt "favored" termination previously observed at spins $43/2^-$ and $51/2^-$ in this nucleus.

ACKNOWLEDGMENTS

This work was in part supported by grants from Atomic Energy of Canada Limited (AECL) Research, the Natural Sciences and Engineering Research Council of Canada, the U.K. Science and Engineering Research Council, and the Swedish Natural Science Research Council.

[1] V.P. Janzen *et al.*, in Proceedings of the International Conference on Nuclear Structure at High Angular Momentum, Ottawa, 1992, edited by J.C. Waddington and D. Ward (AECL Report No. AECL-10613, 1992), Vol. 2 p. 333.

[2] V.P. Janzen, D.R. LaFosse, H. Schnare, D.B. Fossan, A. Galindo-Uribarri, S.M. Mullins, E.S. Paul, L. Persson, S. Pilotte, D.C. Radford, H. Timmers, J.C. Waddington, R. Wadsworth, D. Ward, J.N. Wilson, and R. Wyss, Phys. Rev. Lett. **72**, 1160 (1994).

[3] D.R. LaFosse, D.B. Fossan, J.R. Hughes, Y. Liang, P. Vaska, M.P. Waring, J.-y. Zhang, R.M. Clark, R. Wadsworth, S.A. Forbes, E.S. Paul, V.P. Janzen, A. Galindo-Uribarri, D.C. Radford, D. Ward, S.M. Mullins, D. Prévost, and G. Zwartz, submitted to Phys. Rev. C (1994).

[4] V.P. Janzen, H.R. Andrews, B. Haas, D.C. Radford, D. Ward, A. Omar, D. Prévost, M. Sawicki, P. Unrau, J.C. Waddington, T.E. Drake, A. Galindo-Uribarri, and R. Wyss, Phys. Rev. Lett. **70**, 1065 (1993).

[5] D.R. LaFosse, D.B. Fossan, J.R. Hughes, Y. Liang, P.Vaska, M.P. Waring, and J.-y. Zhang, Phys. Rev. Lett. **69**, 1332 (1992).

[6] R. Wadsworth, H.R. Andrews, R.M. Clark, D.B. Fossan, A. Galindo-Uribarri, V.P. Janzen, J.R. Hughes, D.R. LaFosse, S.M. Mullins, E.S. Paul, D.C. Radford, P. Vaska, M.P. Waring, D. Ward, J.N. Wilson, and R. Wyss, Nucl. Phys. **A559**, 461 (1993).

[7] E.S. Paul, C.W. Beausang, R.M. Clark, R.A. Cunningham, T. Davinson, S.A. Forbes, D.B. Fossan, S.J. Gale, A. Gizon, J. Gizon, K. Hauschild, I.M. Hibbert, A.N. James, P.M. Jones, M.J. Joyce, D.R. LaFosse, R.D. Page, H. Schnare, P.J. Sellin, J. Simpson, R. Wadsworth, M.P. Waring, and P.J. Woods, Phys. Rev. C **48**, R490 (1993).

[8] E.S. Paul, R.M. Clark, S.A. Forbes, D.B. Fossan, J.R. Hughes, D.R. LaFosse, Y. Liang, R. Ma, P.J. Nolan, P.H. Regan, P. Vaska, R. Wadsworth, and M.P. Waring, J. Phys. G **18**, 837 (1992).

[9] M.P. Waring, D.B. Fossan, J.R. Hughes, D.R. LaFosse, Y. Liang, R. Ma, P. Vaska, S.A. Forbes, E.S. Paul, R.M. Clark, and R. Wadsworth, Phys. Rev. C **48**, 2629 (1993).

[10] Y. Liang, D.B. Fossan, J.R. Hughes, D.R. LaFosse, T. Lauritsen, R. Ma, E.S. Paul, P. Vaska, M.P. Waring, N. Xu, and R.A. Wyss, Phys. Rev. C **44**, R578 (1991).

[11] Y. Liang, D.B. Fossan, J.R. Hughes, D.R. LaFosse, T. Lauritsen, R. Ma, E.S. Paul, M.P. Waring, P. Vaska, and N. Xu, Phys. Rev. C **45**, 1041 (1992).

[12] E.S. Paul, J. Simpson, H. Timmers, I. Ali, M.A. Bentley, A.M. Bruce, D.M. Cullen, P. Fallon, and F. Hanna, J. Phys. G **18**, 971 (1992).

[13] E.S. Paul, J. Simpson, S. Araddad, C.W. Beausang, M.A. Bentley, M.J. Joyce, and J.F. Sharpey-Schafer, J. Phys. G **19**, 913 (1993).

[14] D.C. Radford, in *Proceedings of the International Seminar on The Frontier of Nuclear Spectroscopy*, Kyoto, 1992, edited by Y. Yoshizawa, H. Kusakari, and T. Otsuka (World Scientific, Singapore, 1993), p. 229.

[15] D.R. LaFosse, private communication.

[16] T. Bengtsson and I. Ragnarsson, Nucl. Phys. **A436**, 14 (1985).